

# Further mapping of quantitative trait loci for postnatal growth in an intersubspecific backcross of wild *Mus musculus castaneus* and C57BL/6J mice

AKIRA ISHIKAWA<sup>1\*</sup>, SAYURI HATADA<sup>1</sup>, YOSHITAKA NAGAMINE<sup>2</sup>  
AND TAKAO NAMIKAWA<sup>1</sup>

<sup>1</sup>Laboratory of Animal Genetics, Division of Applied Genetics and Physiology, Graduate School of Bioagricultural Sciences, Nagoya University, Chikusa-ku, Nagoya 464-8601, Japan

<sup>2</sup>Department of Animal Breeding and Reproduction, National Institute of Livestock and Grassland Science, Tsukuba 305-0901, Japan

(Received 19 October 2004 and in revised form 24 January 2005)

## Summary

We performed a quantitative trait locus (QTL) analysis of eight body weights recorded weekly from 3 weeks to 10 weeks after birth and two weight gains recorded between 3 weeks and 6 weeks, and between 6 weeks and 10 weeks in an intersubspecific backcross population of wild *Mus musculus castaneus* mice captured in the Philippines and the common inbred strain C57BL/6J (*M. musculus domesticus*), to elucidate the complex genetic architecture of body weight and growth. Interval mapping identified 17 significant QTLs with main effects on 11 chromosomes. In particular, the main effect of the most potent QTL on proximal chromosome 2 increased linearly with age, whereas other QTLs exerted effects on either the early or late growth period. Surprisingly, although wild mice displayed 60% of the body size of their C57BL/6J counterparts, the wild-derived allele enhanced growth at two QTLs. Interestingly, five of the 17 main-effect QTLs identified had significant epistatic interaction effects. Five new epistatic QTLs with no main effects were identified on different chromosomes or regions. For one pair of epistatic QTLs, mice that were heterozygous for the wild-derived allele at one QTL and homozygous for that allele at another QTL exhibited the most rapid growth in all four possible genotypic combinations. Out of the identified QTLs, several showed significant sex-specific effects.

## 1. Introduction

Although several quantitative trait loci (QTLs) have been positionally cloned in animals and plants (e.g. Frary *et al.*, 2000; Grisart *et al.*, 2001; Klein *et al.*, 2004), the actual identity of the polymorphism(s) responsible for the QTL effect remains unknown except for a few cases (Liang *et al.*, 2003). Moreover, the general understanding of the genetic architecture of quantitative variation is poor. Consequently, this area has become one of the grand challenges in current modern biology (Andersson & Georges, 2004).

Body weight in mice has long been used as a model quantitative trait to elucidate the genetic architecture, owing to the ease of measurement throughout life

that can be performed with great accuracy and reliability. To date, many mapping studies have located several QTLs with relatively small phenotypic effects on body weight and growth-related traits, such as obesity, on almost all mouse chromosomes (reviewed by Snyder *et al.*, 2004). However, most previous studies have focused on a single phenotypic measurement recorded at only once during growth, when the maximum phenotypic difference is usually attained between two parental mouse strains used for the construction of a mapping population. Generally, we cannot determine whether the QTLs identified from such a time-fixed mapping study are active at the time of observation or across different growth periods. By contrast, a few studies have evaluated growth using data obtained at different times of the growth process. Morris *et al.* (1999) and Rocha *et al.* (2004) measured body weight at 3 weeks, 6 weeks and 10 weeks after birth. Cheverud *et al.* (1996) and Vaughn *et al.* (1999)

\* Corresponding author. Laboratory of Animal Genetics, Division of Applied Genetics and Physiology, Graduate School of Bioagricultural Sciences, Nagoya University, Chikusa-ku, Nagoya 464-8601, Japan. Tel: +81 52 789 4101. Fax: +81 52 789 4099. e-mail: qtl@nagoya-u.jp

conducted comprehensive QTL analyses of body weights recorded weekly from 1 week to 10 weeks of age. These investigators observed that the number of QTLs for body weight vary from seven at 1 week to 17 at 10 weeks of age, and that QTLs affecting body weight in the early and late growth periods map to different chromosomal locations, indicating a separate genetic system for the two growth periods. This is supported by an index selection experiment in mice for high early postnatal growth, holding later growth constant, and for high later growth, holding early growth constant; this resulted in the establishment of selected lines with identical body-weight phenotypes at 56 days after birth (Atchley *et al.*, 1997). Thus, taking into account the age-specific expression of QTLs in mapping studies might lead to improved understanding of the genetic architecture of growth variation, as highlighted by Atchley & Zhu (1997).

Using the unique intersubspecific backcross population derived from wild *Mus musculus castaneus* mice captured in the Philippines and the common inbred strain, C57BL/6J (*M. musculus domesticus*), we previously reported nine QTLs affecting body weight (Ishikawa *et al.*, 2000; Ishikawa & Namikawa, 2004). Our group has mapped QTLs affecting adult body weight recorded at a single time, at 10 weeks after birth (Ishikawa *et al.*, 2000). Although many QTLs for body weight and growth have been reported, their effects are relatively small and similar to one another (e.g. Cheverud *et al.*, 1996; Morris *et al.*, 1999). Therefore, it is generally difficult to determine the QTLs that are important contributors to complex growth regulation systems. In a recent study, we used two principal components extracted from information on eight body weights recorded weekly from 3 weeks (at weaning) to 10 weeks of age as composite traits to simplify QTL analysis and to identify the key loci contributing significantly to complex growth regulation (Ishikawa & Namikawa, 2004). In the present investigation, we have also mapped several single-trait QTLs affecting body weight at eight different ages and two weight gains. We further analyse the more complex QTL effects, such as age dependency, sex specificity and epistatic interactions, with a view to elucidating the complex genetic architecture of postnatal growth in this unique mouse cross.

## 2. Materials and methods

### (i) *Animals and trait measurements*

The development of the backcross population and details of animal husbandry have been described earlier (Ishikawa *et al.*, 2000). Briefly, a pair of adult wild *M. musculus castaneus* mice of unknown ages were captured live in Luzon Island (The Philippines) and introduced into our laboratory at Nagoya University.

The four wild males obtained from a cross of this pair were mated with eight females of the C57BL/6J inbred strain purchased from Clea Japan (Tokyo, Japan). 34 F<sub>1</sub> females were repeatedly backcrossed to their own wild male parents. In total, 387 backcross mice (186 males and 201 females) from 70 first to third parity litters were produced. Litter size was not standardized at birth to maximize the number of backcross mice reared. Mice were weaned at 3 weeks after birth. Commercial food and tap water were provided *ad libitum*.

Body weights of backcross mice were recorded weekly from 3 weeks to 10 weeks of age to the nearest 0.1 g using a digital balance. Two weight gains (3–6 weeks and 6–10 weeks) were calculated. A total of ten measurements (specifically, eight weekly recorded body weights and two weight gains) were used as quantitative traits in this study (see Table 1 with trait abbreviations). This study conforms to the guidelines for the care and use of laboratory animals of the Graduate School of Bioagricultural Sciences, Nagoya University.

### (ii) *Marker genotyping and linkage map construction*

90 fully informative microsatellite markers spanning all 19 autosomes and the X chromosome were used, which are listed in a previous report (Ishikawa & Namikawa, 2004). Genomic DNA extraction and marker genotyping were performed as described previously (Ishikawa *et al.*, 2000).

Three marker linkage maps were constructed from male, female and sex-combined data with the computer software Map Manager QTXb17 (Manly *et al.*, 2001). Recombination frequencies (%) were converted into genetic distances in cM using the Kosambi map function. The average marker spacing was 20.2 cM in male-specific, 19.5 cM in female-specific and 19.8 cM in sex-averaged linkage maps (Ishikawa & Namikawa, 2004).

### (iii) *QTL analyses*

#### (a) *Exploratory statistical analyses*

Before QTL analyses, the effects of four environmental factors (sex, parity, litter size and litter) on ten growth traits were tested using a linear model of the statistical discovery software JMP (SAS Institute, 2003). The litter involved the combined effect of dam and cage, and was treated as a random effect. The remaining factors were treated as fixed effects. All possible two- and three-way interactions of the fixed effects were additionally included in the model. The fixed and random effects significant at the nominal 5% level were somewhat different, depending on the traits analysed. The effects of sex, litter size and litter

Table 1. Means and standard deviations (SD) in grams for ten growth traits after correction for fixed and random effects and their phenotypic correlations

Trait	Abbreviation	n	Mean ± SD	Wt3	Wt4	Wt5	Wt6	Wt7	Wt8	Wt9	Wt10	G36
Body weight at 3 weeks	Wt3	349	12.9 ± 0.9									
Body weight at 4 weeks	Wt4	352	14.3 ± 1.3	0.80								
Body weight at 5 weeks	Wt5	350	15.2 ± 1.5	0.68	0.85							
Body weight at 6 weeks	Wt6	352	16.6 ± 1.9	0.60	0.73	0.88						
Body weight at 7 weeks	Wt7	352	16.2 ± 1.8	0.58	0.69	0.84	0.93					
Body weight at 8 weeks	Wt8	350	16.6 ± 2.0	0.56	0.66	0.80	0.88	0.95				
Body weight at 9 weeks	Wt9	352	16.8 ± 2.0	0.55	0.65	0.78	0.86	0.93	0.96			
Body weight at 10 weeks	Wt10	352	17.3 ± 2.1	0.55	0.61	0.73	0.81	0.90	0.94	0.96		
Gain from 3 weeks to 6 weeks	G36	349	3.1 ± 1.3	0.08 <sup>ns</sup>	0.36	0.63	0.79	0.75	0.69	0.67	0.61	
Gain from 6 weeks to 10 weeks	G610	352	1.5 ± 1.3	0.10 <sup>ns</sup>	0.01 <sup>ns</sup>	-0.01 <sup>ns</sup>	-0.01 <sup>ns</sup>	0.21	0.35	0.43	0.56	-0.07 <sup>ns</sup>

<sup>ns</sup> Not significant at  $P > 0.05$ ; all other correlations are highly significant at  $P < 1 \times 10^{-4}$ .

were significant for Wt3, Wt4 and G36, those of sex and litter for Wt5–Wt10, and none for G610. Raw data were finally fitted using a model including the fixed effect of sex and litter size, and the random effect of litter for consistent interpretation of the growth data corrected, because no difference was obtained between QTL results from two sets of the data corrected for the individual significant factors and the consistent factors (data not shown). The residuals were standardized for QTL analyses to facilitate the comparison of parameter estimates of detected QTLs between individual traits. Correlation analyses between each pair of the ten growth traits and other general statistical analyses were performed with JMP.

#### (b) Detection of main-effect QTLs

To identify the QTLs with main effects, two methods of interval mapping based on a single QTL model were implemented with the computer software QTL Cartographer Version 1.17 (Basten *et al.*, 2003). One is simple interval mapping (SIM) with a maximum-likelihood method (Lander & Botstein, 1989), and the other is composite interval mapping (CIM) that combines SIM with multiple regression analysis (Zeng, 1993, 1994). By controlling the genetic background containing the other QTLs, CIM can localize QTLs more precisely than SIM (Zeng, 1993, 1994), control for spurious ghost loci (Doerge *et al.*, 1997; Doerge, 2002) and detect multiply linked, sex-specific QTLs (Butterfield *et al.*, 2003). Cofactors that control for the genetic background were chosen by forwards–backwards selection with an acceptance–rejection significance threshold of 1%. A window size of 10 cM was used.

SIM and CIM were performed with 2 cM steps within each interval. The parameter estimates of detected QTLs, such as map positions and additive effects (differences between homozygotes and heterozygotes), were computed using QTL Cartographer. Likelihood of odds (LOD) scores were obtained by dividing the likelihood ratio statistics by 4.605. For the X chromosome of males, the expected additive effect was half the computed value owing to its hemizygous state. The 95% confidence intervals of QTL locations were calculated as described previously (Darvasi & Soller, 1997). The total contribution of all detected main-effect QTLs to phenotypic variance was estimated by summing the square of each additive effect, and dividing it by 4 (Mather & Jinks, 1977). This method leads to overestimation of the total contribution, because a single QTL model is used to detect QTLs and to assess genetic effects. Alternatively, multiple regression analysis of JMP was used to estimate the total contribution. This method leads to underestimation of the total contribution, because sex-specific and closely-linked QTLs,

and QTLs not detected by SIM but by CIM do not provide significant effects in the regression model.

Empirical significance thresholds for both SIM and CIM were established with 1,000 permutations (Churchill & Doerge, 1994) of QTL Cartographer. The computed threshold levels were evaluated as LOD scores.

### (c) Detection of epistatic QTLs

To identify QTLs with epistatic interaction effects, a genome-wide search for all pairs of the 90 marker loci used was performed with Map Manager QTX, based on the assumption that a QTL is positioned at a marker locus. This search is based on a linear regression model with a marker-by-marker interaction term. The difference in the variance between the two models with and without the interaction term was calculated by analysis of variance (ANOVA) of JMP. The total contribution of all detected interactions to the phenotypic variance was estimated by multiple regression analysis of JMP.

To identify significant epistatic QTLs, two tests were performed as described previously (Chmielewicz & Manly, 2002; Ishikawa & Namikawa, 2004). After the total effects of the two loci were tested, the interaction effect was investigated. In the linear model with the interaction term, 1,000 permutations were implemented with Map Manager QTX to test the significance at the genome-wide level. This permutation test provides genome-wide 63%, 5% and 0.1% threshold levels (Chmielewicz & Manly, 2002). However, for consistency with threshold levels used for the above interval mapping, we adopted only the genome-wide 5% threshold level for determining the significance of the total effect. In case the total effect exceeded this threshold, the significance of the interaction effect was examined using the genome-wide thresholds determined for SIM, as described by Knott *et al.* (1998).

### (d) Detection of sex-specific QTLs

To identify QTLs with sex-specific effects, the above interval mapping and epistatic interaction analyses were performed separately for three sex groups (male, female and sex-combined). For interval mapping, it is impossible to investigate an interaction effect of QTL and sex with QTL Cartographer, because the interaction term cannot be included in the software model (Basten *et al.*, 2000). Alternatively, we performed a statistical test to analyse the sex specificity of QTL expression using the web-based software QTL Express (Seaton *et al.*, 2002; <http://qtl.cap.ed.ac.uk/>), which can include the sex effect and QTL-by-sex interactions in the software model (Knott *et al.*, 1998; Quintanilla *et al.*, 2002).

By contrast, sex specificity for epistatic QTLs was examined by three-way ANOVA of JMP, including the interaction term of an interacting marker pair and sex in the model, in view of the assumption described earlier. The Bonferroni-corrected, experiment-wise 5% level was used as a significance threshold.

## 3. Results

### (i) Exploratory statistical analysis

Table 1 shows the phenotypic means and standard deviations for the ten growth traits after correction for fixed and random effects in the intersubspecific backcross population of C57BL/6J and wild *M. musculus castaneus* mice. Correlations between the eight body-weight traits declined with an increase in the age difference between weights. Weight gain in the late growth period from 6 weeks to 10 weeks of age was not significantly correlated with body weight or weight gain in the early growth period from 3 weeks to 6 weeks.

### (ii) QTL analyses

#### (a) Main-effect QTLs

The sex-averaged map was applied in this analysis, because the results of interval mapping of main-effect QTLs were not significantly different between sex-specific and sex-averaged linkage maps. It is thus relatively easy to compare the QTL locations between males and females for detection of sex-specific QTLs.

The empirical significance thresholds used for SIM were determined by permutation and expressed as LOD scores. These were similar among the ten traits and three sex groups: 2.3–2.4 at the genome-wide 10% level, 2.6–2.8 at the genome-wide 5% level and 3.1–3.7 at the genome-wide 1% level.

LOD score profiles for all chromosomes obtained by SIM are depicted in Fig. 1. Ten QTLs with main effects significant at the genome-wide 10% or less level were identified on chromosomes 2, 5, 9, 10, 13, 14, 19 and X. The existence of all ten QTLs detected by SIM was confirmed by CIM. Details of these QTLs are described below, together with CIM data.

The number of cofactors used for CIM was determined separately in each sex group and varied from one to ten, depending on the traits and sex groups. The empirical significance thresholds expressed as LOD scores were not greatly different among the ten traits and three sex groups (2.3–2.6 at the genome-wide 10% level, 2.6–3.0 at the genome-wide 5% level and 3.2–3.7 at the genome-wide 1% level).

CIM results of the ten growth traits are depicted in Table 2. 17 QTLs with main effects were detected on chromosomes 2, 4, 5, 7, 9, 10, 13, 14, 16, 19 and X at

Table 2. QTLs with main effects on growth traits detected by composite interval mapping (CIM)

Chromosome	QTL <sup>a</sup>	Map position <sup>b</sup>	CI <sup>c</sup>	LOD <sup>d</sup>	Additive <sup>e</sup>	% var <sup>f</sup>	Traits affected <sup>g</sup>
2	<i>Pbwg1</i>	D2Mit324 + 0 (33)	17–56	3.1–10.9	0.39–0.71	3.7–12.1	Wt4–Wt10, G36, G610
4	<i>Pbwg2</i>	D4Mit32 – 8 (62)	46	3.1	0.43	3.1	Wt9
5	<i>Pbwg14</i> <sup>F</sup>	D5Mit345 + 0 (1)	76	2.8	0.46	5.1	Wt8
7	<i>Pbwg3</i>	D7Mit259 + 0 (72)	56–78	2.6–3.6	0.33–0.39	2.6–3.7	Wt5–Wt9
9	<i>Pbwg15</i>	D9Mit340 + 2 (43)	62–74	2.6–2.7	0.34–0.37	2.8–3.4	Wt3–Wt4
9	<i>Pbwg4</i>	D9Mit18 – 2 (69)	62	3.0	0.37	3.4	Wt5
10	<i>Pbwg9</i>	D10Mit16 – 2 (14)	48	3.5	–0.42	4.3	G36
10	<i>Pbwg16</i>	D10Mit20 + 10 (45)	35	4.6	0.49	5.9	Wt3
10	<i>Pbwg5</i>	D10Mit145 – 2 (68)	74	2.6	0.34	2.8	Wt7
13	<i>Pbwg17</i>	D13Mit195 – 5 (46)	35–48	4.2–5.1	0.42–0.49	4.4–6.0	Wt6–Wt10
13	<i>Pbwg6</i>	D13Mit195 + 2 (53)	40–48	4.2–4.9	0.42–4.9	4.4–5.3	Wt5–Wt10
14	<i>Pbwg18</i> <sup>F</sup>	D14Mit159 + 0 (30)	42	4.3	0.62	9.4	G610
16	<i>Pbwg19</i> <sup>M</sup>	D16Mit32 + 0 (2)	69	3.0	–0.51	6.5	Wt5
19	<i>Pbwg20</i>	D19Mit29 + 0 (4)	25–62	3.1–6.3	0.37–0.58	3.4–8.2	Wt3–Wt4
X	<i>Pbwg7</i> <sup>M</sup>	DXMit75 – 2 (17)	44–75	3.4–3.8	0.32–0.66	5.5–10.1	Wt5–Wt8, G36
X	<i>Pbwg21</i> <sup>M</sup>	DXMit75 + 8 (27)	43–58	2.6–3.6	0.56–0.65	7.6–10.4	Wt3, G36
X	<i>Pbwg22</i> <sup>F</sup>	DXMit19 – 8 (35)	39–55	2.9–4.3	0.54–0.64	6.9–9.3	Wt9–Wt10

<sup>a</sup> QTL symbol. The superscripts <sup>M</sup> and <sup>F</sup> signify loci with male- and female-specific effects, respectively. The ten QTLs *Pbwg1*, *Pbwg4*–*Pbwg7*, *Pbwg14*, *Pbwg16*, *Pbwg17*, *Pbwg20* and *Pbwg21*, were mapped by both SIM (Fig. 1) and CIM, whereas the remaining seven QTLs were only detected by CIM. The nine QTLs *Pbwg1*–*Pbwg9* have been reported previously (Ishikawa *et al.*, 2000; Ishikawa & Namikawa, 2004).

<sup>b</sup> The positive and negative signs indicate that the QTL maps that distance in cM distal and proximal, respectively, to the nearest marker. The position from the centromere based on the mouse consensus map of the Mouse Genome Database (MGD; <http://www.informatics.jax.org/>) is presented in parentheses.

<sup>c</sup> Minimal and maximal lengths (cM) of 95% confidence intervals calculated from the formula of Darvasi & Soller (1997).

<sup>d</sup> The range of maximum LOD scores.

<sup>e</sup> The range of additive effects in standard-deviation units. The negative sign for *Pbwg9* and *Pbwg19* shows that the wild-derived allele increases the trait value.

<sup>f</sup> The range of percentages of phenotypic variance explained by the QTL.

<sup>g</sup> Traits significant at the genome-wide 10% or less level.

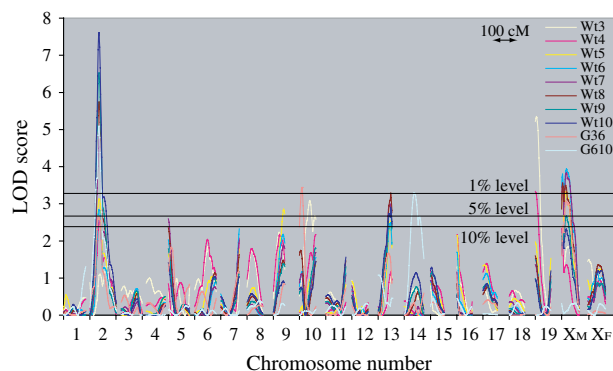


Fig. 1. LOD score plots of QTLs with main effects on postnatal growth. Simple interval mapping (SIM) of eight once-weekly measurements of body weight (Wt3–Wt10) and two weight gains (G36 and G610) (Table 1) was performed with the computer package QTL Cartographer (Basten *et al.*, 2000). The horizontal lines show the genome-wide 10%, 5% and 1% significance levels computed by 1,000 permutations. Map positions in cM were estimated from sex-combined data using Kosambi map function. X<sub>M</sub> and X<sub>F</sub> specify the X chromosome for males and females, respectively.

the genome-wide 5% level. We thus assigned a series of gene symbols (*postnatal body weight growth* (*Pbwg*)) to the QTLs, based on data from an earlier study (Ishikawa & Namikawa, 2004). Of these, nine

QTLs (*Pbwg1*–*Pbwg9*) had been mapped previously (Ishikawa *et al.*, 2000; Ishikawa & Namikawa, 2004) and were reconfirmed in the present single-trait QTL analyses. The other eight QTLs identified in this investigation are all novel.

Six QTLs had sex-specific effects on corresponding traits. QTL-by-sex interactions were significant at the genome-wide 5% level (Table 2). *Pbwg14*, *Pbwg18* and *Pbwg22*, located on chromosomes 5, 14 and X, respectively, were female specific. A male-specific effect was observed for *Pbwg19* on chromosome 16, and *Pbwg7* and *Pbwg21* on the X chromosome.

The 17 QTLs identified accounted for 2.6–12.1% of the total phenotypic variance, depending on the trait (Table 2). The additive effects of *Pbwg9* on chromosome 10 and *Pbwg19* on chromosome 16 were both negative in sign. This finding implies that the wild-derived allele at these two QTLs unexpectedly increases the values for the corresponding traits, although the body size of wild mice is about 60% that of C57BL/6J (Ishikawa *et al.*, 2000). By contrast, the wild mouse allele at all other QTLs decreased trait values.

As depicted in Fig. 2, the 17 QTLs identified were mainly classified into three expression patterns on the basis of changes in maximum LOD scores during

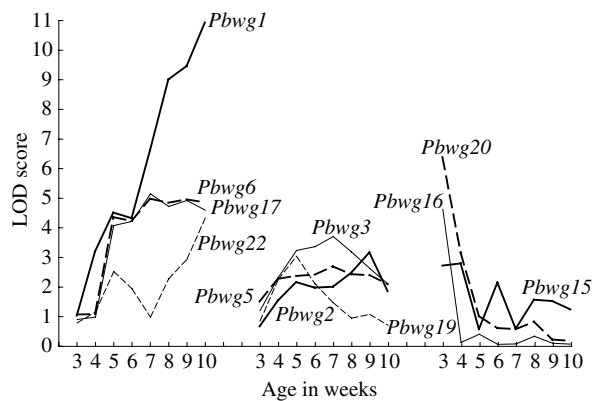


Fig. 2. Changes in maximum LOD scores for detected main-effect QTLs during postnatal growth from 3 weeks to 10 weeks of age. The *Pbwg* codes are the QTL symbols (Table 2). The changes in typical QTLs only are depicted (convex pattern, middle).

postnatal growth. The first pattern was basically characterized by a QTL that displayed an increase in LOD score with age (Fig. 2, left). Four QTLs (*Pbwg1*, *Pbwg6*, *Pbwg17* and *Pbwg22*) displayed a considerable difference in trajectory during growth. *Pbwg1*, which shows the strongest effect of the identified QTLs, displayed a linear increase throughout the entire growth period examined, completely fitting into a simple regression model ( $P < 8.3 \times 10^{-6}$ ). The next pattern was observed for three QTLs (*Pbwg15*, *Pbwg16* and *Pbwg20*) that decreased exponentially with regard to the LOD score during growth (Fig. 2, right). The trajectory of *Pbwg20* was typically fitted into a logarithmic function ( $P < 4.6 \times 10^{-4}$ ). The last pattern was observed for the remaining eight QTLs, which displayed a convex expression pattern during growth (Fig. 2, middle). The trajectory of *Pbwg3* was typically fitted into a quadratic function ( $P < 1.7 \times 10^{-4}$ ).

### (b) Epistatic QTLs

The 5% threshold levels used for testing the significance of total effects in the regression model of Map Manager QTX were determined as 5.2–5.3 (expressed as LOD scores) in three sex groups. For marker-by-marker interaction effects, genome-wide thresholds were approximated as 2.3–2.4, 2.6–2.8, and 3.2–3.7 at the 10%, 5% and 1% levels, respectively.

A genome-wide search for all pairs of the 90 markers used revealed that five marker pairs had epistatic interaction effects on seven body-weight traits, Wt4–Wt10 (Fig. 3). The total effects of the five marker pairs detected greatly exceeded the genome-wide 5% level (LOD = 5.4–9.2) and the marker-by-marker interaction effects exceeded the genome-wide 5% or 1% levels (LOD = 2.8–5.0). Three-way ANOVA

revealed that, apart from the *D2Mit48* and *D9Mit19* pair, the remaining four pairs had highly significant male-specific effects on corresponding traits ( $7.6 \times 10^{-5} < P < 5.1 \times 10^{-3}$ ), greatly exceeding the Bonferroni-corrected 5% level ( $P < 0.05 \div 5 = 0.01$ ). However, only for Wt7, the *D2Mit324* and *D12Mit4* pair (with a *P* value of 0.014) did not exceed this threshold. The epistatic interaction effect of individual pairs accounted for 3.5–12.1% of the total phenotypic variance, depending on traits.

Notably, the chromosomal regions in which epistatic interactions were detected appeared to shift during postnatal growth (Fig. 3). One of the two markers on chromosome 2 showed an interaction with the chromosome 9 marker in the early growth period. In the later period, the other marker on chromosome 2 exhibited an interaction with the chromosome 12 marker. Similar tendencies were evident with regard to the interactions of the two markers on the X chromosome with markers on chromosomes 6 and 13.

In addition, differences in the patterns of the epistatic interactions were clear among the five interacting marker pairs detected, as observed from the age-related changes in LOD score for marker-by-marker interactions (Fig. 4a). The marker pair *D2Mit324* and *D12Mit4* strongly displayed a linear increase throughout the entire growth period, and completely fitted a simple regression line ( $P < 3.1 \times 10^{-5}$ ). The other four pairs exhibited convex patterns with maximum expression at different ages. When the dynamics of the additive effects during growth were traced by a combination of genotypes at interacting marker loci (Fig. 4b), unexpected results were obtained. Generally, mice doubly heterozygous for the wild-derived (C) and C57BL/6J (B) allele at both interacting marker loci were expected to have the largest additive effects in all four possible genotypic combinations, because the wild mice used were smaller than C57BL/6J. However, the additive effect of mice with a B/C genotype at *D4Mit93* and C/C genotype at *D16Mit32* was the largest, with a positive sign throughout the entire growth period examined, indicating that this genotypic combination enhances growth. Moreover, most C/C double homozygotes at all the interacting marker loci did not show the smallest effects. Other genotypic combinations exhibited changes specific for the interaction marker pairs (Fig. 4b).

As shown in Fig. 3, ten epistatic QTLs were identified. A comparison of the map positions of epistatic QTLs (Fig. 3) with those of main-effect QTLs detected above (Table 2) revealed that four QTLs marked by *D2Mit324*, *D9Mit18*, *D16Mit32* and *DXMit75* were identical to the main-effect QTLs, *Pbwg1*, *Pbwg4*, *Pbwg19* and *Pbwg7*, respectively. The QTL marked by *D6Mit74* was previously identified

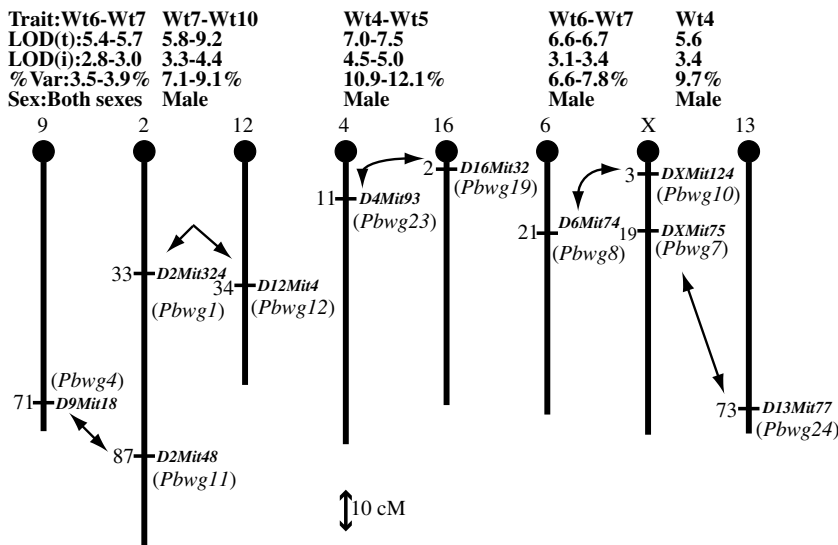


Fig. 3. Chromosomal positions of marker pairs with significant epistatic interaction effects at the genome-wide 5% level. The arrows indicate the interacting marker pairs. The number above the centromere (big closed circle) shows the chromosome number. The number on the left side of the vertical line signifies the map position in cM of the marker from the centromere taken from the mouse consensus map (the Mouse Genome Database, MGD). The QTL symbol is presented in parentheses. ‘Trait’ indicates the traits affected by the interacting marker pair; LOD(t) and LOD(i) are the LOD scores for the total effects and interaction effects, respectively, of the marker pair; %Var indicates the percentage of the phenotypic variance explained by the pair; Sex indicates the sex specificity of the pair.

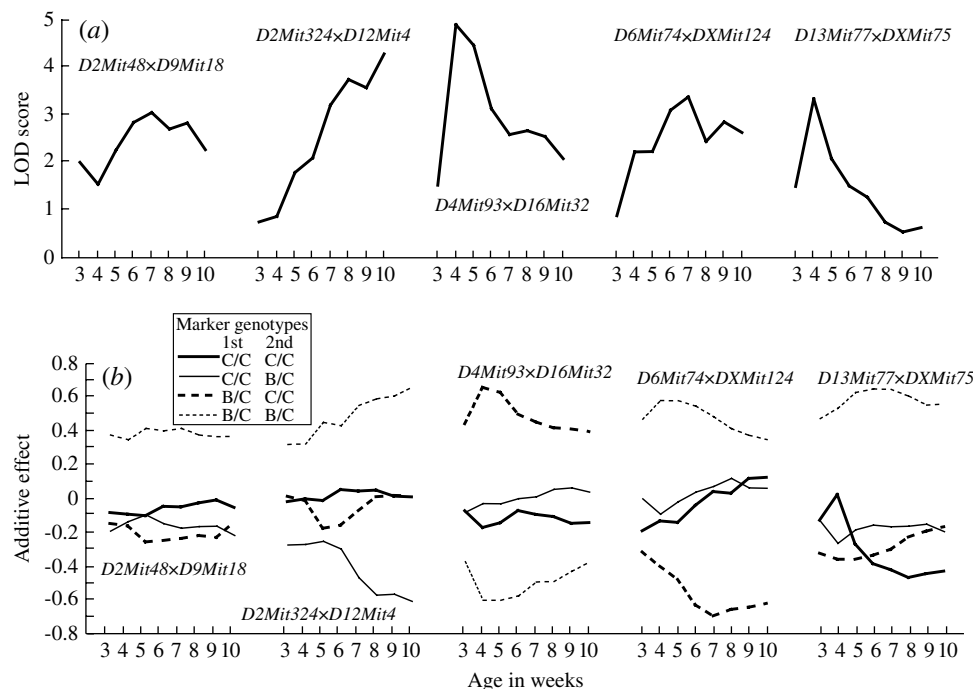


Fig. 4. Age-related changes in LOD scores and additive effects of significant interacting marker pairs. (a) A LOD score for the interaction effect of the interacting marker pair is depicted across growth from 3 weeks to 10 weeks of age. (b) An additive effect in the standard deviation unit is shown for all four possible combinations of genotypes at the interacting marker loci. ‘B’ and ‘C’ denote the marker alleles derived from C57BL/6J and wild *M. musculus castaneus* mice, respectively.

as a main-effect locus, *Pbwg8* (Ishikawa & Namikawa, 2004). Clearly, these five QTLs had both main and epistatic interaction effects on the traits. By contrast, the remaining five QTLs marked by *D2Mit48*,

*D12Mit4*, *D4Mit93*, *D13Mit77* and *DXMit124* mapped to chromosomal regions or chromosomes where no main-effect QTLs were identified (Table 2, Fig. 3), indicating epistatic interaction effects only.

Table 3. Summary of QTLs with main effects and epistatic interaction effects by trait. The average and range are presented in parentheses for each parameter estimate

Trait	Main-effect QTL					Epistatic QTL				
	QTLs	Chromosomes	Additive effect	% var <sup>a</sup>	Total % var <sup>b</sup>	CI	QTLs	Chromosomes	% var <sup>a</sup>	Total % var <sup>b</sup>
Wt3	4	3	0.49 (0.34-0.58)	6.2 (2.9-8.2)	15.2 (25.1)	48 (25-74)	0	0	0	0
Wt4	3	3	0.38 (0.37-0.39)	3.5 (3.4-3.7)	9.7 (10.6)	60 (56-62)	4	4	10.9 (9.7-12.1)	16.8
Wt5	6	6	0.45 (0.37-0.56)	5.1 (3.3-7.7)	23.8 (30.9)	57 (40-69)	2	2	10.9	10.9
Wt6	5	4	0.47 (0.38-0.64)	5.5 (3.5-10.1)	17.8 (28.2)	47 (40-59)	4	4	5.3 (3.9-6.6)	7.5
Wt7	6	5	0.48 (0.34-0.62)	5.8 (2.8-9.2)	20.7 (23.6)	47 (27-74)	6	5	6.1 (3.5-7.8)	17.3
Wt8	6	5	0.47 (0.35-0.63)	5.5 (3.1-9.4)	21.5 (34.4)	54 (21-76)	2	2	8.1	8.1
Wt9	6	5	0.47 (0.33-0.65)	5.9 (2.6-10.3)	17.9 (36.2)	50 (20-78)	2	2	7.6	7.6
Wt10	4	3	0.57 (0.46-0.71)	8.0 (5.3-12.1)	15.2 (33.4)	34 (17-40)	2	2	9.1	9.1
G36	4	3	0.42 (0.41-0.65)	7.0 (4.1-10.4)	9.4 (28.8)	47 (43-51)	0	0	0	0
G610	2	2	0.57 (0.51-0.62)	7.9 (6.4-9.4)	9.6 (16.1)	38 (33-42)	0	0	0	0

<sup>a</sup> Percentage of phenotypic variance explained by each QTL or each pair of epistatic QTLs.

<sup>b</sup> Total percentage of phenotypic variance explained by all QTLs with either main or epistatic effects on the trait. This was estimated by multiple regression analysis and by the method of Mather & Jinks (1977) in parentheses.

Of these, three loci denoted *Pbwig10-Pbwig12* had been mapped previously (Ishikawa *et al.*, 2000; Ishikawa & Namikawa, 2004). The remaining two loci were assigned new gene symbols (Fig. 3).

(c) Cross-sectional analysis of identified QTLs

The above QTL results are longitudinally presented across growth. To understand the genetic architecture of postnatal growth from a cross-sectional point of view, we have summarized the number of detected QTLs with main and epistatic interaction effects, and the magnitudes of parameter estimates and phenotypic contributions for the QTLs by trait (Table 3). The number of main-effect QTLs and chromosomes containing QTLs were not greatly different among traits, except for the weight gain trait G610, which had the smallest numbers of both main-effect QTLs and chromosomes. Similarly, the average of the additive effect and proportion of phenotypic variance explained by each QTL did not differ considerably among traits.

By contrast, a clear tendency was observed for epistatic QTLs (Table 3). Although no epistatic QTLs were discovered for three traits (Wt3, G36 and G610), the number of epistatic QTLs detected was greater in the early growth period, with a boundary at around 7 weeks of age. This reflected the differences in the total contribution of all detected epistatic QTLs to phenotypic variance.

4. Discussion

Upon inclusion of a previously-mapped epistatic QTL (*Pbwig13*) on distal chromosome 5 (Ishikawa & Namikawa, 2004), which was not detected in the present study, our intersubspecific backcross using the unique wild *M. musculus castaneus* mouse revealed that the genetic architecture of postnatal growth is affected by 24 QTLs located on 13 chromosomes with relatively small effects (~12% of the phenotypic variance). The 24 QTLs can be classified into three categories depending on their effects on postnatal growth: 11 QTLs with main effects only (*Pbwig2*, *Pbwig3*, *Pbwig5*, *Pbwig14-Pbwig18* and *Pbwig20-Pbwig22*), six QTLs with epistatic interaction effects only (*Pbwig10-Pbwig13*, *Pbwig23* and *Pbwig24*) and seven QTLs with both types of effects (*Pbwig1*, *Pbwig4*, *Pbwig6-Pbwig9* and *Pbwig19*). Furthermore, investigation of the expression dynamics of the 17 main-effect QTLs identified revealed that few of these affect the entire growth process. A typical example is the most potent QTL, *Pbwig1* on chromosome 2, which affects the entire growth process, in contrast to other QTLs, which affect either early or late growth. This supports previous findings that early and late growth in mice occur under different genetic

regulation (Cheverud *et al.*, 1996; Vaughn *et al.*, 1999; Rocha *et al.*, 2004). A similar finding has additionally been reported for chicken growth (Carlborg *et al.*, 2003).

Several statistical methods have been reported for mapping epistatic QTLs (e.g. Kao *et al.*, 1999; Cheverud, 2000; Sen & Churchill, 2001; Yi *et al.*, 2003; Carlborg & Haley, 2004). The simplest method is to perform two-way ANOVA or to use the general linear model (GLM) of variance analysis for all marker pairs, as we performed here and other investigators previously reported (Brockmann *et al.*, 2000; Rocha *et al.*, 2004). However, there are issues of difficult resolution in the use of this type of two-locus model (Cheverud, 2000; Goodnight, 2000; Nelson *et al.*, 2001). To assess the validity of our epistatic QTLs, we implemented a multiple-interval mapping (MIM) based on a multiple-QTLs model (Kao *et al.*, 1999) with the software QTL Cartographer. MIM confirmed the presence of all main-effect QTLs identified here, except *Pbwg5* and *Pbwg17*. By contrast, no epistatic QTLs were identified. This negative result was not unexpected, because all the pairs of our epistatic QTLs were composed of interactions between loci with and without main effects. Yi *et al.* (2003) highlighted that it is difficult for MIM with an expectation-maximization algorithm to identify epistatic QTLs without main effects. We have, in fact, confirmed this disadvantage of MIM for different quantitative traits in mice (A. Ishikawa *et al.*, unpublished). Thus, alternative approaches based on Bayesian methods (e.g. Yi *et al.*, 2003) are required to detect epistatic QTLs with no main effects.

Many epistatic QTLs affecting growth and obesity have been reported in different mouse crosses (Routman & Cheverud, 1997; Brockmann *et al.*, 2000; Cheverud *et al.*, 2001; Rocha *et al.*, 2004; Yi *et al.*, 2004). Interactions between QTLs with and without main effects are detected in intercrosses of LG/J and SM/J (Routman & Cheverud, 1997), and DU6I and DBA/2 (Brockmann *et al.*, 2000) mouse strains. In the BSB backcross population from a cross of C57BL/6J and *M. spretus*, Yi *et al.* (2004) reported strong interactions between loci on chromosomes 2 and 12 for adult body weight and obesity traits, and showed that chromosome 2 has a very weak main effect, which cannot be detected using non-epistatic models. In the present study, we show the strongest interaction for the same combinations of chromosomes. The location of our chromosome-12 QTL, *Pbwg12*, with no main effect, coincides with that of the locus reported by Yi *et al.* (2004), but the locations of the two chromosome-2 QTLs are evidently different. The locations of other four epistatic QTLs, *Pbwg4*, *Pbwg7*, *Pbwg11* and *Pbwg23* (on chromosomes 2, 4, 9 and X), coincide with those reported previously (Routman & Cheverud, 1997; Brockmann

*et al.*, 2000) but the magnitudes of the main effects and locations of the interacting counterparts are different. To avoid false positives in the identification of epistatic QTLs, we adopted a highly stringent threshold (the genome-wide 5% level). Therefore, in addition to the above coincidences with regard to map location, all ten identified epistatic QTLs exceeding the stringent threshold must be genuine and are unlikely to be statistical artefacts.

Our results showed that the contribution of epistasis is more pronounced in the early growth period. Unfortunately, no such observations on epistatic QTLs have been reported in mice. However, our findings are in concordance with those of Carlborg *et al.* (2003), who performed QTL mapping of body weights at different ages in chickens and revealed that epistasis is important for early growth characterized by the development of internal organs, but less important for late growth involving the main deposition of body tissues.

Using a formal statistical test, we obtained significant evidence of sex specificity for six main-effect QTLs on chromosomes 5, 14, 16 and X. Vaughn *et al.* (1999) reported a male-specific QTL for growth on chromosome 16 that maps close to our male-specific QTL *Pbwg19*. Three male-specific QTLs affecting body weight on the X chromosome (Dragani *et al.*, 1995; Brockmann *et al.*, 1998) were detected in the regions containing our male-specific *Pbwg7* and *Pbwg21*. However, to date, few studies have investigated the sex-specific effects of epistatic interactions for body weight and its related traits in mice. Only Cheverud *et al.* (2001) reported male- or female-specific interaction effects on adiposity and tail length. In the present investigation, four pairs of epistatic QTLs exhibited male-specific effects on growth. Of these, three epistatic QTLs (*Pbwg7*, *Pbwg8* and *Pbwg19*) displayed the same direction of sex specificity for main effects, as shown presently as well as in a previous study (Ishikawa & Namikawa, 2004). By contrast, *Pbwg1* on chromosome 2 exerted a main effect on both sexes but exhibited a male-specific interaction effect. We cannot rule out the possibility that *Pbwg1* comprises two or more tightly linked loci, because the dissection of a single QTL with a large effect into multiple QTLs with small effects has been previously reported in mice (Podolin *et al.*, 1998; Legare *et al.*, 2000; Wang *et al.*, 2003).

The biological mechanisms underlying sex-specific QTLs remain unclear. However, as discussed previously (Ishikawa & Namikawa, 2004), our sex-specific QTLs might be dependent on the presence of sex hormones or influenced by genes on the Y chromosome. In addition, growth traits are sexually dimorphic in general. Such a phenotype is expected if the causative gene of a growth QTL is highly expressed and/or active in gonadal tissue, as in the

case of *Nr1f-2* (current symbol *Zfp369* (zinc-finger protein 369)), a sex-limited QTL candidate for physical dependence on ethanol on mouse chromosome 13 (Marshall *et al.*, 2002).

Several QTLs affecting growth and obesity traits have been reported (reviewed by Snyder *et al.*, 2004) and many growth-related functional genes have been listed in databases such as the Mouse Genome Database. We identified several previously reported QTLs and candidate genes within the 95% confidence intervals of our QTLs. As the confidence intervals obtained from this kind of QTL mapping are evidently very broad (17–78 cM in the present case), comparisons of QTL map positions identified in the present study with previous analyses are problematic and questionable (Ishikawa & Namikawa, 2004). We used wild *M. musculus castaneus* mice captured in the Philippines, whereas most previous studies used common laboratory strains (Snyder *et al.*, 2004) originally derived from a small pool of ancestors (Nishioka, 1995; Guenet & Bonhomme, 2003) for the construction of mapping populations. Therefore, our QTLs contributing to naturally occurring variations in postnatal growth are expected to be novel, or most of our QTL alleles might be new, even though the map positions are identical to those of previous QTLs. Fine mapping of our QTLs is required to reduce the number of potential candidates that remain within the intervals.

In conclusion, using the unique intersubspecific backcross of wild *M. musculus castaneus* mice and C57BL/6J, we have mapped many QTLs for postnatal growth. We have further revealed the complex nature of the QTL effects (epistatic interactions, sex specificity and age dependence) involved in the regulation of postnatal growth in mice. We are currently constructing congenic strains for some of the identified QTLs to obtain biological evidence of the complex QTL effects and to pinpoint the specific QTLs.

This work was supported, in part, by a Grant-in-Aid for Scientific Research from the Japan Society for the Promotion of Science.

## References

- Andersson, L. & Georges, M. (2004). Domestic animal genomics: deciphering the genetics of complex traits. *Nature Reviews Genetics* **5**, 202–212.
- Atchley, W. R. & Zhu, J. (1997). Developmental quantitative genetics, conditional epigenetic variability and growth in mice. *Genetics* **147**, 765–776.
- Atchley, W. R., Xu, S. & Cowley, D. E. (1997). Altering developmental trajectories in mice by restricted index selection. *Genetics* **146**, 629–640.
- Basten, C. J., Weir, B. S. & Zeng, Z.-B. (2003). *QTL Cartographer Version 1.17*. Raleigh, North Carolina: Department of Statistics, North Carolina State University.
- Brockmann, G. A., Haley, C. S., Renne, U., Knott, S. A. & Schwerin, M. (1998). Quantitative trait loci affecting body weight and fatness from a mouse line selected for extreme high growth. *Genetics* **150**, 369–381.
- Brockmann, G. A., Kratzsch, J., Haley, C. S., Renne, U., Schwerin, M., & Karle, S. (2000). Single QTL effects, epistasis, and pleiotropy account for two-thirds of the phenotypic  $F_2$  variance of growth and obesity in DU6i × DBA/2 mice. *Genome Research* **10**, 1941–1957.
- Butterfield, R. J., Roper, R. J., Rhein, D. M., Melvold, R. W., Haynes, L., Ma, R. Z., Doerge, R. W. & Teuscher, C. (2003). Sex-specific quantitative trait loci govern susceptibility to Theiler's murine encephalomyelitis virus-induced demyelination. *Genetics* **163**, 1041–1046.
- Carlborg, O. & Haley, C. S. (2004). Epistasis: too often neglected in complex trait studies? *Nature Reviews Genetics* **5**, 618–625.
- Carlborg, O., Kerje, S., Schütz, K., Jacobsson, L., Jensen, P. & Andersson, L. (2003). A global search reveals epistatic interaction between QTL for early growth in the chicken. *Genome Research* **13**, 413–421.
- Cheverud, J. M. (2000). Detecting epistasis among quantitative trait loci. In *Epistasis and the Evolutionary Process* (ed. J. B. Wolf, E. D. Brodie III & M. J. Wade), pp. 58–81. Oxford, UK: Oxford University Press.
- Cheverud, J. M., Routman, E. J., Duarte, F. A. M., van Swinderen, B. & Cothran, K. (1996). Quantitative trait loci for murine growth. *Genetics* **142**, 1305–1319.
- Cheverud, J. M., Vaughn, T. T., Pletscher, L. S., Peripato, A. C., Adams, E. S., Erikson, K. J. & King-Ellison, K. J. (2001). Genetic architecture of adiposity in the cross of LG/J and SM/J inbred mice. *Mammalian Genome* **12**, 3–12.
- Chmielewicz, K. M. & Manly, K. F. (2002). *User Manual for QTX, revised for QTXb17*. Buffalo, New York: Roswell Park Cancer Institute.
- Churchill, G. A. & Doerge, R. W. (1994). Empirical threshold values for quantitative trait mapping. *Genetics* **138**, 963–971.
- Darvasi, A. & Soller, M. (1997). A simple method to calculate resolving power and confidence interval of QTL map location. *Behavior Genetics* **27**, 125–132.
- Doerge, R. W. (2002). Mapping and analysis of quantitative trait loci in experimental populations. *Nature Reviews Genetics* **3**, 43–52.
- Doerge, R. W., Zeng, Z.-B. & Weir, B. S. (1997). Statistical issues in the search for genes affecting quantitative traits in experimental populations. *Statistical Science* **12**, 195–219.
- Dragani, T. A., Zeng, Z.-B., Canzian, F., Gariboldi, M., Ghilarducci, M. T., Manenti, G. & Pierotti, M. A. (1995). Mapping of body weight loci on mouse chromosome X. *Mammalian Genome* **6**, 778–781.
- Frary, A., Nesbitt, T. C., Esbitt, A., Frary, A., Grandillo, S., van der Knaap, E., Cong, B., Lui, J., Meller, J., Elber, R., Aipert, K. B. & Tanksley, S. D. (2000). *fw2.2*: a quantitative trait locus key to the evolution of tomato fruit size. *Science* **289**, 85–88.
- Goodnight, C. J. (2000). Quantitative trait loci and gene interaction: the quantitative genetics of meta-populations. *Heredity* **84**, 587–598.
- Grisart, B., Coppieters, W., Farnir, F., Karim, L., Ford, C., Berzi, P., Cambisano, N., Mni, M., Reid, S., Simon, P., Spelman, R., Georges, M. & Snell, R. (2001). Positional candidate cloning of a QTL in dairy cattle: identification of a missense mutation in the bovine *DGAT1* gene with major effect on milk yield and composition. *Genome Research* **12**, 222–231.

- Guenet, J. & Bonhomme, F. (2003). Wild mice: an ever-increasing contribution to a popular mammalian model. *Trends in Genetics* **19**, 24–31.
- Kao, C. H., Zeng, Z.-B. & Teasdale, R. D. (1999). Multiple interval mapping for quantitative trait loci. *Genetics* **152**, 1203–1216.
- Klein, R. F., Allard, J., Avnur, Z., Nikolcheva, T., Rotstein, D., Carlos, A. S., Shea, M., Waters, R. V., Belknap, J. K., Peltz, G. & Orwoll, E. S. (2004). Regulation of bone mass in mice by the lipoxigenase gene *ALOX15*. *Science* **303**, 229–232.
- Knott, S. A., Marklund, L., Haley, C. S., Andersson, K., Davies, W., Ellegren, H., Fredholm, M., Hansson, I., Hoyheim, B., Lundstrom, K., Moller, M. & Andersson, L. (1998). Multiple marker mapping of quantitative trait loci in a cross between outbred wild boar and Large White pigs. *Genetics* **149**, 1069–1080.
- Ishikawa, A. & Namikawa, T. (2004). Mapping major quantitative trait loci for postnatal growth in an inter-subspecific backcross between C57BL/6J and Philippine wild mice by using principal component analysis. *Genes and Genetic Systems* **79**, 27–39.
- Ishikawa, A., Matsuda, Y. & Namikawa, T. (2000). Detection of quantitative trait loci for body weight at 10 weeks from Philippine wild mice. *Mammalian Genome* **11**, 824–830.
- Lander, E. S. & Botstein, D. (1989). Mapping Mendelian factors underlying quantitative traits using RFLP linkage maps. *Genetics* **121**, 184–199.
- Legare, M. E., Bartlett, F. S. & Frankel, W. N. (2000). A major effect QTL determined by multiple genes in epileptic EL mice. *Genome Research* **10**, 42–48.
- Liang, T., Spence, J., Liu, L., Strother, W. N., Chang, H. W., Ellison, J. A., Lumeng, L., Li, T.-K., Foroud, T. & Carr, L. G. (2003).  $\alpha$ -Synuclein maps to a quantitative trait locus for alcohol preference and is differentially expressed in alcohol-preferring and -nonpreferring rats. *Proceedings of the National Academy of Sciences of the USA* **100**, 4690–4695.
- Manly, K. F., Cudmore, Jr, R. H. & Meer, J. M. (2001). Map Manager QTX, cross-platform software for genetic mapping. *Mammalian Genome* **12**, 930–932.
- Mather, K. & Jinks J. L. (1977). *Introduction to Biometrical Genetics*. London, UK: Chapman and Hall.
- Marshall, K. E., Godden, E. L., Yang, F., Burgers, S., Buck, K. J. & Sikela, J. M. (2002). *In silico* discovery of gene-coding variants in murine quantitative trait loci using strain-specific genome sequence databases. *Genome Biology* **3**, 1–9.
- Morris, K. H., Ishikawa, A. & Keightley, P. D. (1999). Quantitative trait loci for growth traits in C57BL/6J X DBA/2J mice. *Mammalian Genome* **10**, 225–228.
- Nelson, M. R., Kardina, S. L., Ferrell, R. E. & Sing, C. F. (2001). A combinatorial partitioning method to identify multi-locus genotypic partitions that predict quantitative trait variation. *Genome Research* **11**, 458–470.
- Nishioka, Y. (1995). The origin of common laboratory mice. *Genome* **38**, 1–7.
- Podolin, P. L., Denny, P., Armitage, N., Lord, C. J., Hill, N. J., Levy, E. R., Peterson, L. B., Todd, J. A., Wicker, L. S. & Lyons, P. A. (1998). Localization of two insulin-dependent diabetes (Idd) genes to the Idd10 region on mouse chromosome 3. *Mammalian Genome* **9**, 283–286.
- Quintanilla, R., Milan, D. & Bidanel, J.-P. (2002). A further look at quantitative trait loci affecting growth and fatness in a cross between Meishan and Large White pig populations. *Genetics Selection Evolution* **34**, 193–210.
- Rocha, J. L., Eisen, E. J., van Vleck, L. D. & Pomp, D. (2004). A large-sample QTL study in mice: I. Growth. *Mammalian Genome* **15**, 83–99.
- Routman, E. J. & Cheverud, J. M. (1997). Gene effects on a quantitative trait: two-locus epistatic effects measured at microsatellite markers and at estimated QTL. *Evolution* **51**, 1654–1662.
- SAS Institute (2003). *JMP User's Guide, Version 5.1*. Cary, North Carolina: SAS Institute.
- Seaton, G. S., Haley, C. S., Knott, S. A., Kearsley, M. & Visscher, M. (2002). QTL express: mapping quantitative trait loci in simple and complex pedigrees. *Bioinformatics* **18**, 339–340.
- Sen, S. & Churchill, G. A. (2001). A statistical framework for quantitative trait mapping. *Genetics* **159**, 371–387.
- Snyder, E. E., Walts, B., Perusse, L., Chagnon, Y. C., Weisnagel, S. J., Rankinen, T. & Bouchard, C. (2004). The human obesity gene map: the 2003 update. *Obesity Research* **12**, 369–439.
- Vaughn, T. T., Pletscher, L. S., Peripato, A., King-Ellison, K., Adams, E., Erikson, C. & Cheverud, J. M. (1999). Mapping quantitative trait loci for murine growth: a closer look at genetic architecture. *Genetical Research* **74**, 313–322.
- Wang, X. S., Le Roy, I., Nicodeme, E., Li, R. H., Wagner, R., Petros, Churchill, G. A., Harris, S., Darvasi, A., Kirilovsky, J., Roubertoux, P. L. & Paigen, B. (2003). Using advanced intercross line for high-resolution mapping of HDL cholesterol quantitative trait loci. *Genome Research* **13**, 1654–1664.
- Yi, N., Xu, S. & Allison, D. B. (2003). Bayesian model choice and search strategies for mapping interacting quantitative trait loci. *Genetics* **165**, 867–883.
- Yi, N., Diament, A., Chiu, S., Kim, K., Allison, D. B., Fislser, J. S. & Warden, C. H. (2004). Characterization of epistasis influencing complex spontaneous obesity in the BSB model. *Genetics* **167**, 399–409.
- Zeng, Z.-B. (1993). Theoretical basis for separation of multiple linked gene effects in mapping quantitative trait loci. *Proceedings of the National Academy of Sciences of the USA* **90**, 10972–10976.
- Zeng, Z.-B. (1994). Precision mapping of quantitative trait loci. *Genetics* **136**, 1457–1468.